Geared photochemistry

an interdependent heterogeneous near-infrared catalytic system using up-conversion glass and g-CN for CuAAC chemistry

Kocaarslan, Azra; Sumer, Isik; Esen, Cansu; Kumru, Baris; Eryurek, Gonul; Yagci, Yusuf

DOI
10.1039/d2py01075e

Publication date
2022

Document Version
Final published version

Published in
Polymer Chemistry

Citation (APA)
Kocaarslan, A., Sumer, I., Esen, C., Kumru, B., Eryurek, G., & Yagci, Y. (2022). Geared photochemistry: an interdependent heterogeneous near-infrared catalytic system using up-conversion glass and g-CN for CuAAC chemistry. *Polymer Chemistry*, *13*(46), 6393-6399. https://doi.org/10.1039/d2py01075e

Polymer
Chemistry

ROYAL SOCIETY
OF CHEMISTRY

PAPER

View Article Online
View Journal | View Issue

Cite this: *Polym. Chem.*, 2022, **13**, 6393

Geared photochemistry: an interdependent heterogeneous near-infrared catalytic system using up-conversion glass and g-CN for CuAAC chemistry†

Azra Kocaarslan,[a] Isik Sumer,[b] Cansu Esen,[c] Baris Kumru,[c,d] Gonul Eryurek[b] and Yusuf Yagci *[a]

Received 19th August 2022,
Accepted 26th October 2022

DOI: 10.1039/d2py01075e

rsc.li/polymers

From the synthesis of small biomolecules to complex macromolecular structures, click chemistry is one of the most promising and straightforward methodologies owing to its easy accessibility and high efficiency. A dual-heterogeneous photocatalyst with the capability of engendering light emission in upconversion materials combined with graphitic carbon nitride (g-CN) could present a powerful tool in electron transfer reactions, specifically in copper-catalyzed azide–alkyne cycloaddition (CuAAC) click reactions. We herein describe a "geared photochemistry" approach for producing an electron from g-CN by in-source lightening in the near-infrared region using upconversion glass that produces copper(I) to initiate the click reaction. Using this approach, the photocatalytic activation of g-CN has been achieved by using Tm^{3+} and Yb^{3+} ion-doped zinc-tellurite glass which absorbs laser irradiation at 975 nm and is capable of emitting blue light at 475 nm. The efficiency of this system has been investigated for various CuAAC reactions ranging from small molecule synthesis to the macromolecular scale including modification strategies of polymers.

Introduction

The 1,3-dipolar cycloaddition reaction between terminal alkynes and azides is a superior organic reaction and an easier way to synthesize 1,2,3-triazole derivatives. After Sharpless and Meldal introduced the copper complex to the click concept, it became a landmark in synthetic chemistry.[1,2] Simple reactions with a high yield under mild conditions without the need for purification, stability to a variety of solvents including water, and leniency of most functional groups make the 1,3-dipolar cycloaddition between azides and alkynes a model reaction of click chemistry.[3] Since then, numerous studies have been conducted toward obtaining an in-depth understanding of click reaction phenomena.[4] Due to the versatile application possibility of this reaction, it has been used in many research fields from biomolecule synthesis[5–7] to drug discovery[8] and polymer chemistry[9–14] to materials science.[15] Most of these studies rely on the copper-catalyzed azide–alkyne cycloaddition reaction (CuAAC) activated by a copper(I) salt towards regioselectivity. The required copper(I) species for the reaction can be furnished indirectly by several approaches.[16] To date, there have been many touchstone reports on the issue including the photochemical process which is the most promising way of generating copper(I).[17,18] The light-induced CuAAC concept involves the *in situ* reduction of air-stable copper(II) species to the desired active copper(I) species by a photochemical redox process.[19] This process is achieved either by (i) direct reduction of $CuCl_2$/ligand complexes or (ii) indirect reduction by the photochemically generated active species such as free radicals or carbocations. For the accomplishment of CuAAC reactions, the redox potential of the copper complex and the photochemically generated radicals are critical. The photoinduced CuAAC approach also provides the possibility of combining the process with chain polymerizations to form complex macromolecular structures.[20,21]

Alternatively, the energy required to reduce metal complexes can be provided by visible light irradiation of photocatalysts such as graphitic carbon nitride (g-CN) and polynuclear aromatic compounds.[22–24] Among two-dimensional

---

[a] *Department of Chemistry, Faculty of Science and Letters, Istanbul Technical University, 34469 Maslak, Istanbul, Turkey. E-mail: yusuf@itu.edu.tr*
[b] *Department of Physics Engineering, Faculty of Science and Letters, Istanbul Technical University, 34469 Maslak, Istanbul, Turkey*
[c] *Department of Colloid Chemistry, Max Planck Institute of Colloids and Interfaces, Am Mühlenberg 1, 14476 Potsdam, Germany*
[d] *Aerospace Structures & Materials Department, Faculty of Aerospace Engineering, Delft University of Technology, Kluyverweg 1, 2629 HS Delft, Netherlands*

† Electronic supplementary information (ESI) available. See DOI: **https://doi.org/10.1039/d2py01075e**

photocatalysts, g-CN possesses exceptional features such as good thermal stability, recyclability and high catalytic activity.[25,26] This visible light-sensitive metal-free semiconductor can be easily synthesized *via* thermal condensation of nitrogen-rich and abundant organic monomers at 550 °C.[27] g-CN stands for a family of materials where many parameters such as porosity, light absorption, surface charge, dispersibility and elemental ratio can be adjusted.[28] In a typical semiconductor, photocatalytically formed excited electrons and holes enable the photoredox cycle to address a rich variety of reactions.[29] g-CN has been widely investigated in photocatalytic reactions such as CO_2 reduction[30] and water splitting;[31] yet in the synthesis of polymers[32] and in organic chemistry,[24] g-CN catalyzed photoinduced reactions are used as well. Moreover, once irradiated, g-CN can show low reactivity under dark conditions due to the trapping of electrons in its mesoporous structure.[33] As the activity of g-CN is restricted in the visible range,[34] the utilization of lower energy light sources (such as near infrared, NIR) is desired. For this reason, a combination of light upconversion (UC) systems with g-CN possesses great potential for NIR activation. Typically, the conversion of NIR radiation into visible light is achieved *via* thermometry,[35,36] optical fibers, optical data storage, quantum information, bioimaging, bioanalyses, and white light sources.[37–44] In this connection, it is worth mentioning that when photochromic groups are attached to the surface of UC nanoparticles, certain reactions can be induced directly in the NIR region without taking advantage of visible light emission.[45,46]

The UC method involves nonlinear optical processes characterized by the successive absorption of two or more photons for the emission of radiation at shorter wavelengths. Selection of host materials as well as the selection of rare earth (RE) ions affects the energy distribution of the UC emission. Generally, Yb^{3+} is used as a sensitizer in RE-doped materials because its absorption of NIR radiation occurs over a wide energy range *via* the transition from the ground state ($^2F_{7/2}$) to the excited state ($^2F_{5/2}$) which splits into Stark levels when doped in a glass matrix. Tellurite glasses synthesized using various modifiers such as ZnO, K_2O, BaO, GeO_2, Nb_2O_5, and B_2O_3 are suitable host materials for RE ions and have unique physical and chemical properties that make them useful for a wide range of technical applications. They exhibit a wide range of optical transparency from the mid-infrared to ultraviolet region, a high refractive index, a low melting temperature, and good chemical and mechanical stability.[47,48] Previous spectroscopic studies have confirmed that codoped TeO_2-based glasses with Yb^{3+} and Tm^{3+}, Er^{3+}, Pr^{3+}, Nd^{3+}, Sm^{3+} and Ho^{3+} result in a higher absorption coefficient, UC-emission quantum efficiencies, stimulated emission cross-sections and relatively low luminescence concentration quenching.[49–53]

The generation of UC and white light (WL) in both singly and doubly doped tellurite glasses with various RE ions (including Tm^{3+} and Yb^{3+}/Tm^{3+} ions) has been reported.[54–57] It has been shown that environmental conditions, such as pressure, excitation power, the concentration of dopant ions in the matrix, and so on, affect both UC and WL efficiencies. WL is described by blue, green, and red colors, which are its fundamental components.[58–63] The UC process may trigger the generation of visible light and WL from infrared radiation by suitable lanthanide ions or combinations of them.

In this work, we report a "geared photochemistry" approach for the NIR induced CuAAC click reaction by the sequential combination of NIR absorption, visible emission of UCG and electron release followed by reduction of the $CuCl_2$/ligand to essentially form a copper(I) catalyst.

Results and discussion

The initial focus of this study was the generation of blue light emission of Yb^{3+}/Tm^{3+} doubly doped TeO_2-ZnO glass *via* the absorption of NIR radiation. The method used for the synthesis of the sample was the conventional melt-quenching technique. The optical absorption spectrum of the zinc-tellurite glass was measured between the range of 400–2000 nm in order to identify the absorption lines of Yb^{3+} and Tm^{3+} ions (Fig. 1a). The absorption lines centered at around 465, 685, 780, 1210, and 1710 nm were identified as the Tm^{3+} transitions to the $^1G_4$, $^3F_2$ + $^3F_3$, $^3H_4$, $^3H_5$, and $^3F_4$ levels from its $^3H_6$ ground level. On the other hand, a broad absorption band centred at about 975 nm appears in the spectrum due to the

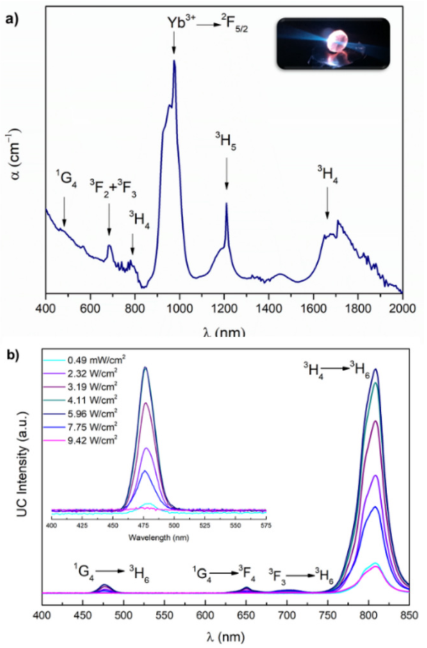

Fig. 1 (a) Absorption spectra of Yb^{3+} and Tm^{3+} doped zinc-tellurite glass, recorded at room temperature. (b) Emission spectra of Yb^{3+} and Tm^{3+} doped zinc-tellurite glass under 975 nm laser excitation with different pumping powers.

transition from the $^{2}F_{7/2}$ ground state to the $^{2}F_{5/2}$ excited state of the Yb^{3+} ions. Excitation power-dependent emission peaks of the glass are shown separately in Fig. 1b.

The emission peaks of Tm^{3+} ions in the zinc-tellurite glass were observed at 525, 547 and 670 nm in the visible region. These peaks correspond to the $^{1}G_{4} \rightarrow {}^{3}H_{6}$, $^{4}F_{2,3} \rightarrow {}^{3}H_{6}$, and $^{3}F_{4} \rightarrow {}^{3}H_{6}$ energy transitions, respectively. The UC emission intensities of all three emissions increased with increasing excitation power in the 0.49 W cm^{-2} to 7.75 W cm^{-2} range. The colour analyses in Fig. 2 indicate the weak dependence of the colour coordinates (CIE-1976) on the altered laser excitation power. The results of the colour coordinates (x; y) on the excitation power of the laser light at 975 nm wavelength were found to be (0.17, 0.28), (0.18, 0.28) and (0.19, 0.30) for 0.49 W cm^{-2}, 4.11 W cm^{-2} and 7.75 W cm^{-2}, respectively.

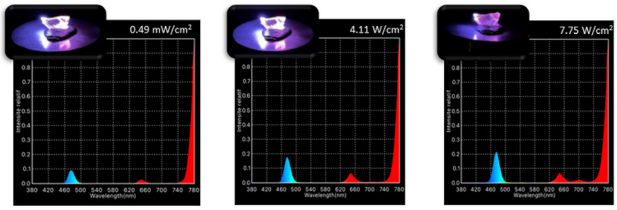

Fig. 2 Emission-related luminescence spectra of Yb^{3+} and Tm^{3+} doped zinc-tellurite glass under 975 nm laser excitation with different pumping powers.

As shown in Fig. 3a, laser source irradiation at 975 nm enables a possible energy transfer between the corresponding ions in the UC glass which gives rise to blue light emissions. This *in situ* emission excites mpg-CN (mesoporous graphitic carbon nitride) and generates an electron–hole pair. After the charge separation, the copper(II) complex in the reaction medium is reduced by an electron and turns into copper(I)

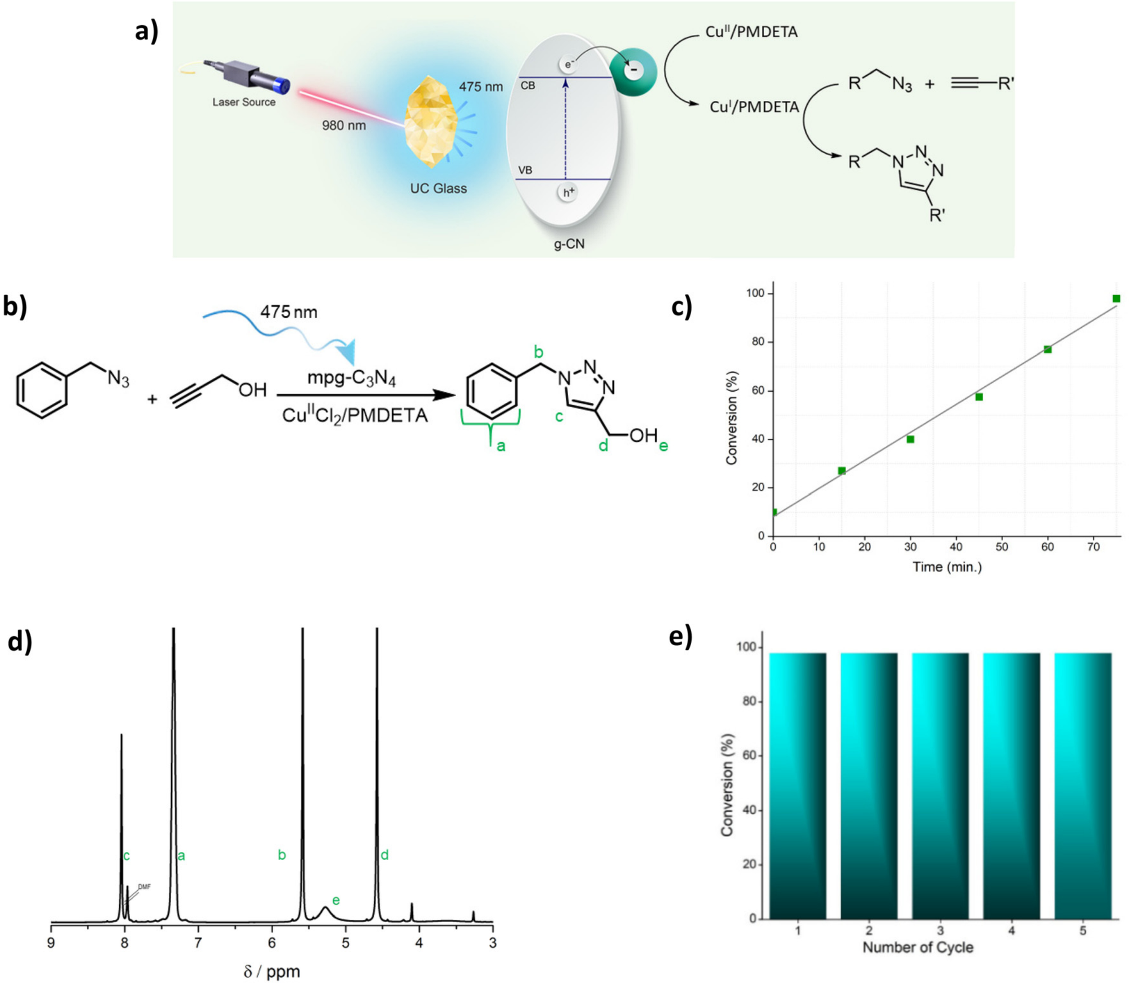

Fig. 3 (a) Visual demonstration of the geared reaction. The sequential system activates the $CuCl_2$ complex to initiate the click reaction under NIR light irradiation with the combination of g-CN and UCG. (b) Proposed mechanism of the copper catalyzed click reaction between benzyl azide and propargyl alcohol. (c) ^{1}H NMR spectrum of the CuAAC click reaction between benzyl azide and propargyl alcohol. (d) Conversion–time plot of the CuAAC click reaction as measured by ^{1}H NMR spectroscopy through integration of the benzylic protons around 5.5 ppm. (e) Evolution of the catalytic activity of recycled g-CN.

which is required for catalyzing the cycloaddition reaction between the azide and alkyne groups.

g-CN photocatalysts used in this work have been fully characterized (see the ESI†). The corresponding UV absorption spectra of g-CN photocatalysts and copper salts are given in Fig. S7†, which confirm that the corresponding photo-induced electron transfer process is initiated exclusively by the excitation of the UCG. As demonstrated, g-CN photocatalysts exhibit photocatalytic activity in which blue light is emitted from the UCG at 475 nm, while the copper salts are unaffected by light in this region. Thus, the click reaction does not proceed in the absence of a photocatalyst.

Firstly, we studied a model reaction between benzyl azide and propargyl alcohol in the presence of $CuCl_2$/PMDETA, mpg-CN, and UCG (Fig. 3b). The reaction was simultaneously tracked by ^1H NMR spectroscopy. While the UCG was excited at 975 nm with a laser source, it emitted blue light at 475 nm due to the Tm^{3+} ions within. This emitted light engenders the g-CN activation in the reaction medium to release electrons which are required to reduce the $CuCl_2$ complex to form copper(I) for the click reaction. The kinetic profile was followed by ^1H NMR and the appearance of a new peak at around 5.5 ppm confirmed the greatly performed click reaction within 2 h (Fig. 3b–d). The recyclability of g-CN was also studied; the experimental result shows that g-CN could be used up to five times in CuAAC click reactions as a part of the dual system (Fig. 3e). Subsequently, the study was extended to various alkyne compounds.

Table 1 shows that the system worked well for all alkyne derivatives, progressing to complete conversion within 2 h (Fig. S8–12†). The reaction between benzyl azide and aromatic alkyne derivatives proceeded relatively slowly but produced a high yield in a short time. Additionally, the functional group tolerance was investigated by using anthracene derivatives as an azide source with the cycloaddition reaction showing high efficiency. Furthermore, another up-converting type catalyst, organodispersible carbon nitride (CMp-VTA), which absorbs at relatively longer wavelengths was also tested. Notably, high yields were attained under identical experimental conditions (Table 1, entry 1).

The success of the reaction with low molar mass compounds led to the extension of the approach to macromol-

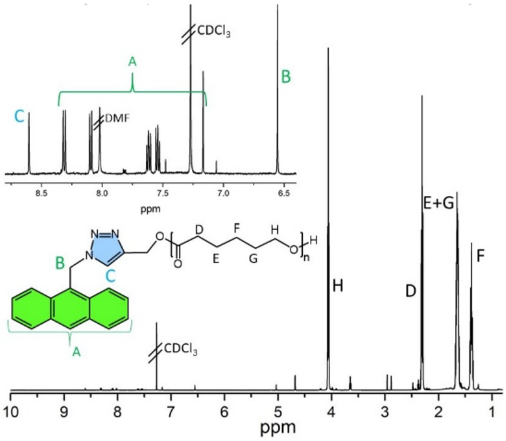

Fig. 4 ^1H NMR spectrum of anthracene functional poly(ε-caprolactone) (yield 56%).

Table 1 NIR light-triggered photocatalytic system for the CuAAC reaction in the presence of $CuCl_2$/PMDETA and g-CN photocatalysts between various azide and alkyne compounds[a]

Run	Photocatalyst	Azide	Alkyne	Products	Conv.[b] (%)
1[c]	CMp-vTA	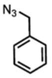	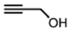	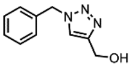	98
2[c]	mpg-CN	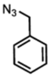	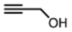	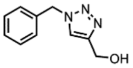	98
3[c]	mpg-CN	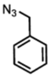	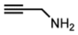	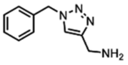	90
4[d]	mpg-CN	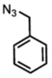	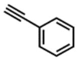	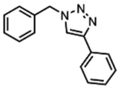	98
5[d]	mpg-CN	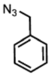	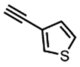	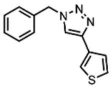	98
6[e]	mpg-CN	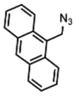	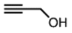	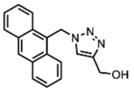	90

[a] All reactions were carried out in DMSO-d_6 at room temperature. [b] Conversions were determined by ^1H NMR spectroscopy. [c] Reaction time = 2 h. [d] Reaction time = 8 h. [e] Reaction time = 4 h.

ecular synthesis. For this purpose, alkyne functional poly(ε-caprolactone) (PCL) was modified with anthracene. The corresponding ^{1}H NMR spectrum shows the characteristic peaks which identify the anthracene functionality (Fig. 4). Spectroscopic studies were also conducted (Fig. S13 and 14†). The fluorescence spectrum of anthracene functionalized PCL clearly indicates end group modification by emission bands of the excited (singlet) anthracene at 595, 655, and 725 nm.

Additionally, click reactions between macromolecular chains were studied. Thus, azide functional polystyrene (PS-N_3) and alkyne functional poly(ε-caprolactone) (PCL-alkyne) were used as antagonist click functional polymers to form block copolymers with structurally different segments. The overall mechanism is shown in Fig. 5 with the corresponding GPC spectra of the polymers. The GPC analysis clearly indicates an increase in the molecular weight and the presence of a shoulder refers to a starting polystyrene moiety arising from the presence of a small amount of the non-functional precursor (Fig. 5b). The characteristic peaks that identify the triazole ring are seen in the corresponding ^{1}H NMR spectrum (Fig. S15†).

In order to extend the macromolecular aspect, the possibility of photoinduced crosslinking by the described approach was also tested. Fig. 6 shows the pathway of the successful crosslinking reaction upon irradiation of multifunctional click components with a 875 nm laser in the presence of mpg-CN and $CuCl_2$/PMDETA under open air conditions. The gelation was completed after 2 hours. The FTIR spectra of the corresponding starting materials and the final product are presented in Fig. 7. As can be seen, the azide peak at 2100 cm^{-1} significantly decreased as a consequence of triazole ring formation.

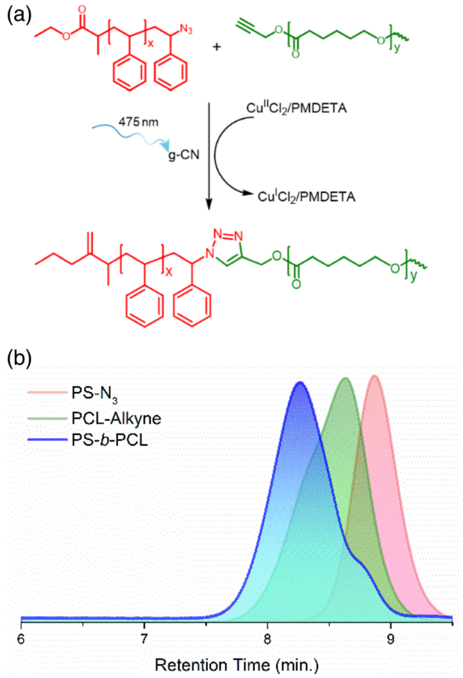

Fig. 5 (a) Schematic diagram of block copolymer formation. (b) GPC traces of PS-N_3 (M_n = 1900 g mol^{-1}), PCL-alkyne (M_n = 4266 g mol^{-1}) and PS-*b*-PCL block copolymers (M_n = 6171 g mol^{-1}).

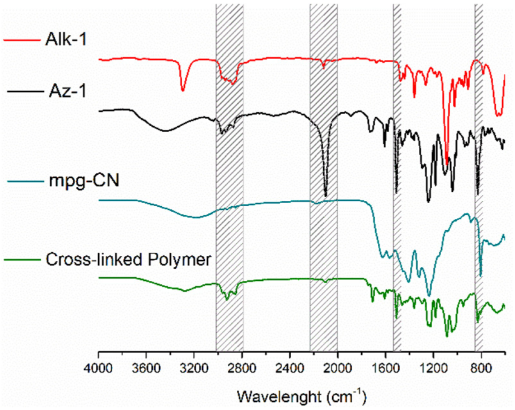

Fig. 7 FTIR spectra of Alk-1, Az-1, mpg-CN and the cross-linked polymer.

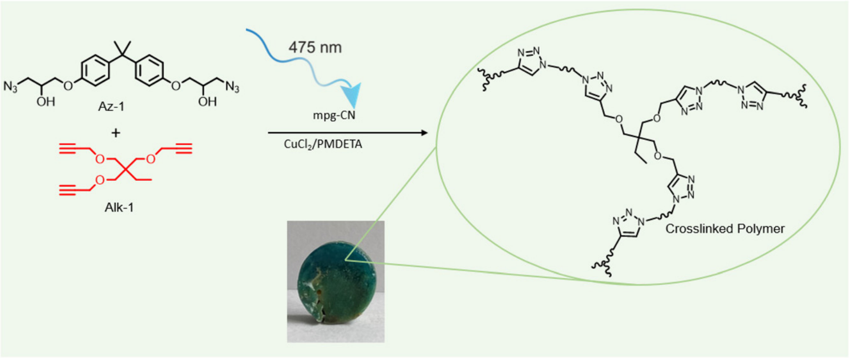

Fig. 6 Proposed mechanism for the NIR induced photo-crosslinking process.

Conclusion

The Tm^{3+} and Yb^{3+} ion-doped zinc-tellurite UCG can activate g-CN with the aid of an internally light emitting process. For the CuAAC process, the visible light excitation of g-CN by the emitted light from NIR light triggered the UCG in the presence of $CuCl_2$ generated active copper(I) species to catalyze a click reaction. In this study, an interdependent heterogeneous system by using UCG in conjunction with g-CN under NIR light is presented, offering a highly effective click methodology for (macro)molecules in synthetic chemistry. The combined use of graphitic carbon and UCG allowed the system to be successfully used several times due to the nature of heterogeneous catalysts.

Author contributions

A. K. contributed to the synthesis and characterization of small molecules and macromolecules. I. S. and G. E. contributed to the synthesis and characterization of up-conversion glass. C. E. and B. K. contributed to the synthesis and characterization of graphitic carbon nitride. Y. Y. supervised the study and was responsible for writing the grant on which the study is based. All authors contributed to manuscript preparation and editing.

Conflicts of interest

The authors declare no competing interests.

Acknowledgements

The authors acknowledge the funding from The Scientific and Technological Research Council of Turkey (TUBITAK), project number: 120C121.

References

1 H. C. Kolb, M. Finn and K. B. Sharpless, *Angew. Chem., Int. Ed.*, 2001, **40**, 2004–2021.

2 C. W. Tornøe, C. Christensen and M. Meldal, *J. Org. Chem.*, 2002, **67**, 3057–3064.

3 V. V. Rostovtsev, L. G. Green, V. V. Fokin and K. B. Sharpless, *Angew. Chem.*, 2002, **114**, 2708–2711.

4 P. Kalra, R. Kaur, G. Singh, H. Singh, G. Singh, G. Kaur and J. Singh, *J. Organomet. Chem.*, 2021, **944**, 121846.

5 Q. Wang, T. R. Chan, R. Hilgraf, V. V. Fokin, K. B. Sharpless and M. Finn, *J. Am. Chem. Soc.*, 2003, **125**, 3192–3193.

6 H. Sun and K. S. Schanze, *ACS Appl. Mater. Interfaces*, 2022, **14**(18), 20506–20519.

7 R. E. Bird, S. A. Lemmel, X. Yu and Q. A. Zhou, *Bioconjugate Chem.*, 2021, **32**, 2457–2479.

8 M. Finn, H. C. Kolb and K. B. Sharpless, *Nat. Synth.*, 2022, **1**, 8–10.

9 W. Xi, H. Peng, A. Aguirre-Soto, C. J. Kloxin, J. W. Stansbury and C. N. Bowman, *Macromolecules*, 2014, **47**, 6159–6165.

10 J. A. Johnson, M. Finn, J. T. Koberstein and N. J. Turro, *Macromol. Rapid Commun.*, 2008, **29**, 1052–1072.

11 K. Ma, X. Jin, W. Gan, C. Fan and H. Gao, *Polym. Chem.*, 2022, **13**, 891–897.

12 K. Sunitha and C. R. Nair, in *Handbook of Thermoset Plastics*, Elsevier, 2022, pp. 931–952.

13 X. Li and Y. Xiong, *ACS Omega*, 2022, **7**(42), 36918–36928.

14 A. J. Anderson, E. Grey, N. J. Bongiardina, C. N. Bowman and S. J. Bryant, *Biomacromolecules*, 2021, **22**, 1127–1136.

15 J. E. Moses and A. D. Moorhouse, *Chem. Soc. Rev.*, 2007, **36**, 1249–1262.

16 M. A. Tasdelen and Y. Yagci, *Angew. Chem., Int. Ed.*, 2013, **52**, 5930–5938.

17 S. Dadashi-Silab and Y. Yagci, *Tetrahedron Lett.*, 2015, **56**, 6440–6443.

18 B. D. Fairbanks, L. J. Macdougall, S. Mavila, J. Sinha, B. E. Kirkpatrick, K. S. Anseth and C. N. Bowman, *Chem. Rev.*, 2021, **121**, 6915–6990.

19 S. C. Ritter and B. König, *Chem. Commun.*, 2006, 4694–4696.

20 S. Doran and Y. Yagci, *Polym. Chem.*, 2015, **6**, 946–952.

21 S. Doran, G. Yilmaz and Y. Yagci, *Macromolecules*, 2015, **48**, 7446–7452.

22 C. Kütahya, Y. Yagci and B. Strehmel, *ChemPhotoChem*, 2019, **3**, 1180–1186.

23 M. Arslan, G. Yilmaz and Y. Yagci, *Polym. Chem.*, 2015, **6**, 8168–8175.

24 S. Dadashi-Silab, B. Kiskan, M. Antonietti and Y. Yagci, *RSC Adv.*, 2014, **4**, 52170–52173.

25 M. Jia, M. Cai, X. Wang, Y. Fang, W. Cao, Y. Song, L. Yuan, Y. Chen and L. Dai, *Mol. Catal.*, 2022, **518**, 112067.

26 R. Sharma, M. Almáši, S. P. Nehra, V. S. Rao, P. Panchal, D. R. Paul, I. P. Jain and A. Sharma, *Renewable Sustainable Energy Rev.*, 2022, **168**, 112776.

27 J. Zhu, P. Xiao, H. Li and S. A. Carabineiro, *ACS Appl. Mater. Interfaces*, 2014, **6**, 16449–16465.

28 Z. Zhao, Y. Sun and F. Dong, *Nanoscale*, 2015, **7**, 15–37.

29 Y. Zheng, L. Lin, B. Wang and X. Wang, *Angew. Chem., Int. Ed.*, 2015, **54**, 12868–12884.

30 J. Lin, W. Tian, H. Zhang, X. Duan, H. Sun and S. Wang, *Energy Fuels*, 2020, **35**, 7–24.

31 S. Wang, J. Zhang, B. Li, H. Sun and S. Wang, *Energy Fuels*, 2021, **35**, 6504–6526.

32 N. Yandrapalli, T. Robinson, M. Antonietti and B. Kumru, *Small*, 2020, **16**, 2001180.

33 G. Chen, Z. Zhang, W. Zhang, L. Xia, X. Nie, W. Huang, X. Wang, L. Wang, C. Hong and Z. Zhang, *Mater. Horiz.*, 2021, **8**, 2018–2024.

34 B. Kumru, D. Cruz, T. Heil and M. Antonietti, *Chem. Mater.*, 2020, **32**, 9435–9443.

35 S. Tabanli and G. Eryurek, *Sens. Actuators, A*, 2019, **285**, 448–455.

36 M. Erdem, O. Erguzel, M. K. Ekmekci, H. Orucu, H. Cinkaya, S. Genc, A. Mergen, G. Eryurek and B. Di Bartolo, *Ceram. Int.*, 2015, **41**, 12805–12810.

37 B. Strehmel, C. Schmitz, T. Bromme, A. Halbhuber, D. Oprych and J. S. Gutmann, *J. Photopolym. Sci. Technol.*, 2016, **29**, 111–121.

38 J. Lalevée, H. Mokbel and J.-P. Fouassier, *Molecules*, 2015, **20**, 7201–7221.

39 J. Lalevée, N. Blanchard, M. A. Tehfe, M. Peter, F. Morlet-Savary and J. P. Fouassier, *Macromol. Rapid Commun.*, 2011, **32**, 917–920.

40 S. Wu, J. P. Blinco and C. Barner-Kowollik, *Eur. J. Chem.*, 2017, **23**, 8325–8332.

41 R. Liu, H. Chen, Z. Li, F. Shi and X. Liu, *Polym. Chem.*, 2016, **7**, 2457–2463.

42 F. Wang, D. Banerjee, Y. Liu, X. Chen and X. Liu, *Analyst*, 2010, **135**, 1839–1854.

43 G. Yang, L. Zhu, J. Hu, H. Xia, D. Qiu, Q. Zhang, D. Zhang and G. Zou, *Eur. J. Chem.*, 2017, **23**, 8032–8038.

44 Z. Chen, D. Oprych, C. Xie, C. Kutahya, S. Wu and B. Strehmel, *ChemPhotoChem*, 2017, **1**, 499–503.

45 Z. Li, J. Zhu, X. Guan, R. Liu and Y. Yagci, *Macromol. Rapid Commun.*, 2019, **40**, 1900047.

46 A. Bagheri, H. Arandiyan, C. Boyer and M. Lim, *Adv. Sci.*, 2016, **3**, 1500437.

47 S. Cenk, B. Demirata, M. Öveçoglu and G. Özen, *Spectrochim. Acta, Part A*, 2001, **57**, 2367–2372.

48 A. T. Gorgulu, H. Cankaya, A. Kurt, A. Speghini, M. Bettinelli and A. Sennaroglu, *J. Lumin.*, 2012, **132**, 110–113.

49 J. Zhou, Q. Liu, W. Feng, Y. Sun and F. Li, *Chem. Rev.*, 2015, **115**, 395–465.

50 F. Auzel, *Chem. Rev.*, 2004, **104**, 139–174.

51 M. Haase and H. Schäfer, *Angew. Chem., Int. Ed.*, 2011, **50**, 5808–5829.

52 S. Tabanli, G. Bilir and G. Eryurek, *J. Lumin.*, 2017, **182**, 146–153.

53 F. Xu, Y. Zhao, M. Hu, P. Zhang, N. Kong, R. Liu, C. Liu and S. K. Choi, *Chem. Commun.*, 2018, **54**, 9525–9528.

54 H. Zijlmans, J. Bonnet, J. Burton, K. Kardos, T. Vail, R. Niedbala and H. Tanke, *Anal. Biochem.*, 1999, **267**, 30–36.

55 S. Wu and H. J. Butt, *Adv. Mater.*, 2016, **28**, 1208–1226.

56 X. Sun, J. Sun, B. Dong, G. Huang, L. Zhang, W. Zhou, J. Lv, X. Zhang, M. Liu and L. Xu, *Biomaterials*, 2019, **201**, 42–52.

57 M. K. Hossain, M. I. Khan and A. El-Denglawey, *Appl. Mater. Today*, 2021, **24**, 101104.

58 G. Bilir, A. Kaya, H. Cinkaya and G. Eryürek, *Spectrochim. Acta, Part A*, 2016, **165**, 183–190.

59 M. Runowski, N. Stopikowska, S. Goderski and S. Lis, *J. Alloys Compd.*, 2018, **762**, 621–630.

60 Q. Guo, J. Wu, Y. Yang, X. Liu, J. Jia, J. Dong, Z. Lan, J. Lin, M. Huang and Y. Wei, *J. Power Sources*, 2019, **426**, 178–187.

61 Z. Sun, Z. Fu and G. Liu, *J. Lumin.*, 2019, **206**, 176–184.

62 S. Shi, L.-D. Sun, Y.-X. Xue, H. Dong, K. Wu, S.-C. Guo, B.-T. Wu and C.-H. Yan, *Nano Lett.*, 2018, **18**, 2964–2969.

63 H. Zhang, Z.-H. Chen, X. Liu and F. Zhang, *Nano Res.*, 2020, **13**, 1795–1809.